Electronic Supplementary Information

A temperature-dependent tricoloured mechanochromic fluorescent material with polymorphic structures

Xinghong Zhang,[a] Shuang Yuan,[a] Yunxiang Lu,[b] Haichuang Lan,[a] Shuzhang Xiao,[a*] Tao Yi [c*]

a Hubei Key Laboratory of Natural Products Research and Development, College of Biological and Pharmaceutical Sciences, China Three Gorges University, Yichang 443002, Hubei, P. R. China.

b Key Laboratory for Advanced Materials and Department of Chemistry, East China University of Science and Technology, Shanghai 200237, P. R. China.

c State Key Laboratory for Modification of Chemical Fibers and Polymer Materials, College of Chemistry, Chemical Engineering and Biotechnology, Donghua University, Shanghai 201620, P.R. China

Contents

1. Synthesis

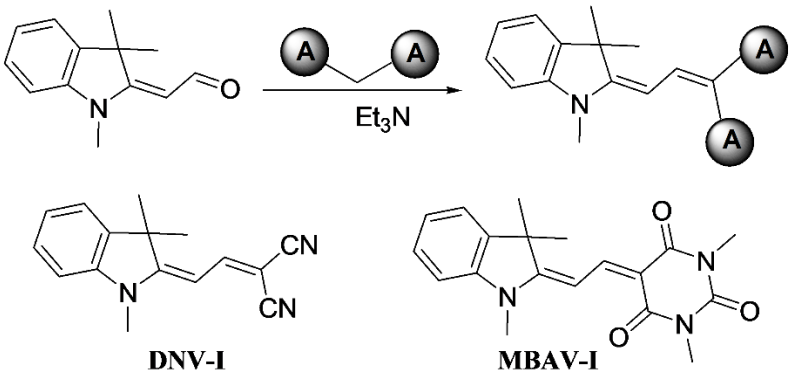

Scheme S1. Synthesis of target D-π-A molecules

General procedure: Fisher aldehyde (1 eq), malononitrile (or barbituric acid or 1,3-dimethylbarbituric acid,1eq), and Et_3N (1.2 eq) were dissolved in ethanol (30 mL) and heated to reflux for 2 hours. After cooled to room temperature, the precipitated yellow solid was collected by suction filtration, and then subjected to column chromatography to provide target compounds.

DNV-I: Yield: 48%. ^{1}H NMR (400 MHz, $CDCl_3$) δ 7.84 (d, *J* = 13.5 Hz, 1H), 7.34 (td, *J* = 7.8, 1.2 Hz, 1H), 7.29 (d, *J* = 6.9 Hz, 1H), 7.16 (td, *J* = 7.5, 0.7 Hz, 1H), 6.97 (d, *J* = 7.9 Hz, 1H), 5.85 (d, *J* = 13.5 Hz, 1H), 3.41 (s, 3H), 1.61 (s, 6H). HRMS: calcd for $C_{16}H_{15}N_3Na$ $[M+Na]^+$ 272.1164, found 272.1155. [1]

MBAV-I: Yield: 50%. ^{1}H NMR (400 MHz, $CDCl_3$) δ 8.73 (d, *J* = 14.5 Hz, 1H), 7.60 (d, *J* = 14.5 Hz, 1H), 7.36 (dd, *J* = 12.1, 4.2 Hz, 2H), 7.21 (t, *J* = 7.4 Hz, 1H), 7.04 (d, *J* = 7.8 Hz, 1H), 3.55 (s, 3H), 3.38 (d, *J* = 4.8 Hz, 6H), 1.73 (s, 6H). HRMS: calcd for $C_{19}H_{22}N_3O_3$ $[M+H]^+$ 340.1661, found 340.1653.[2]

2. Polymorph Prediction

Table S1. Molecular packing of predicted polymorph of **DNV-I**

Space group	Molecular packing	Intermolecular π-π interaction between π dimer	Energy (kcal/mol)
C2	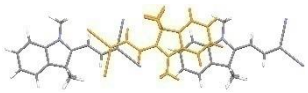	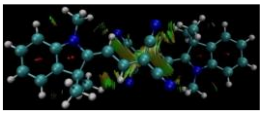	21.14
C2/c	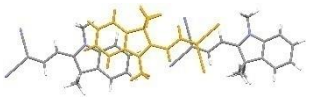	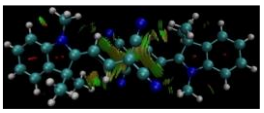	21.09
Cc	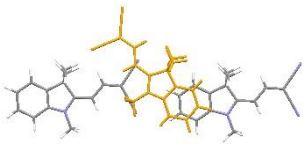	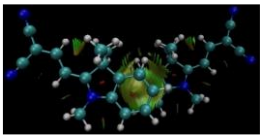	22.68
P-1	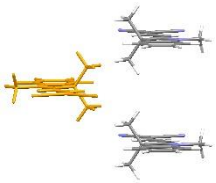	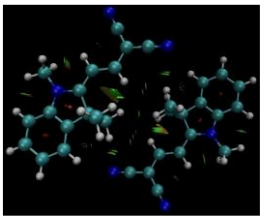	20.87
P2₁	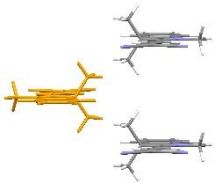	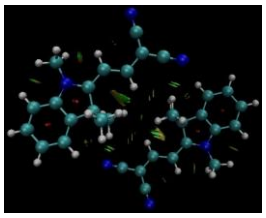	20.87
P2₁/c	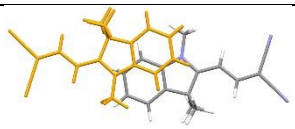	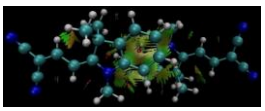	20.87
P2₁2₁2₁		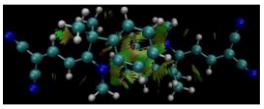	21.78
Pbca		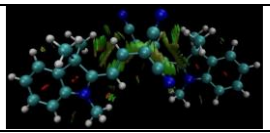	21.20
Pbcn		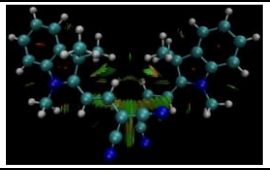	23.83
Pna2₁	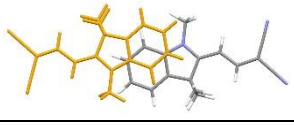	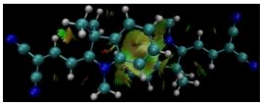	22.24

Table S2. Molecular packing of predicted polymorph of **MBAV-I**

Space group	Molecular packing	Intermolecular π-π interaction	Energy (kcal/mol)
C2		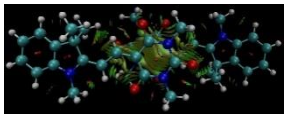	48.93
C2/c		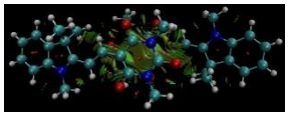	48.93
Cc	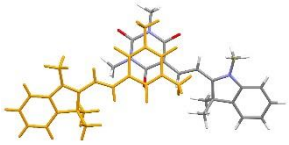	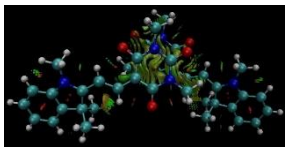	51.78
P-1		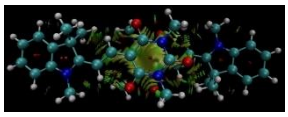	46.95
P2₁		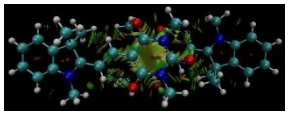	46.95
P2₁/c		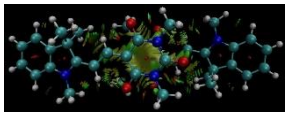	46.95
P2₁2₁2₁		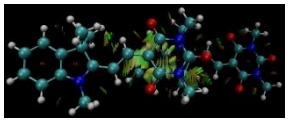	51.92
Pbca	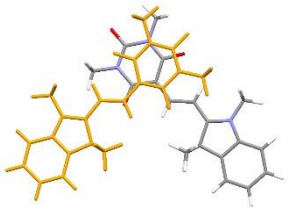	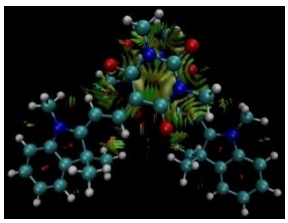	46.88
Pbcn		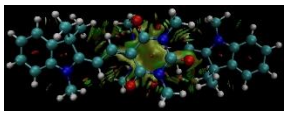	50.10
Pna2₁	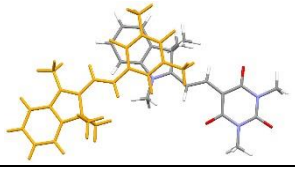	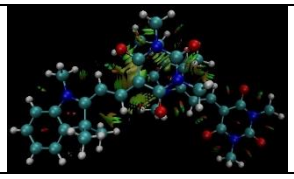	52.78

***Note**: For **MBAV-I**, only the most intense intermolecular π-π interactions between π dimers are analyzed and visualized for clarity.*

3. DFT calculation and photophysical properties

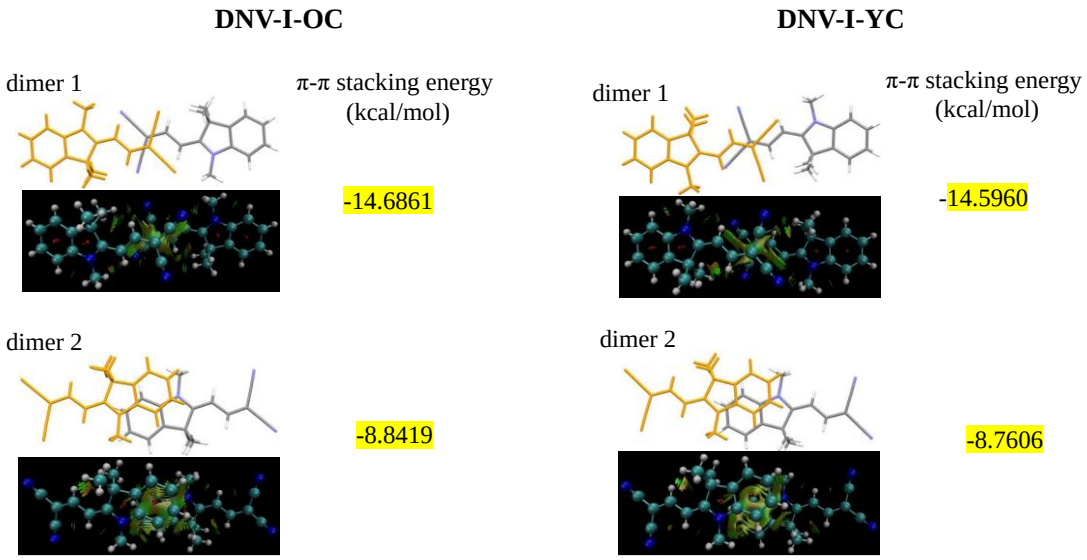

Fig. S1. Intermolecular π-π interactions in the single crystals of **DNV-I**

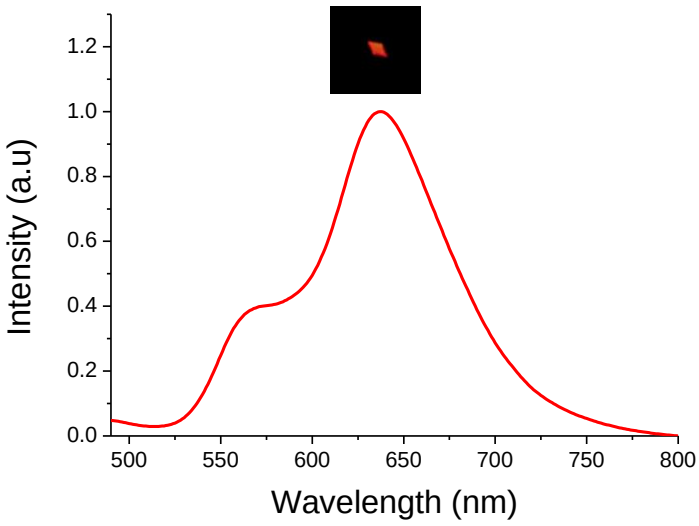

Fig. S2. Fluorescent spectrum and image of the red-emissive crystal of **DNV-I**

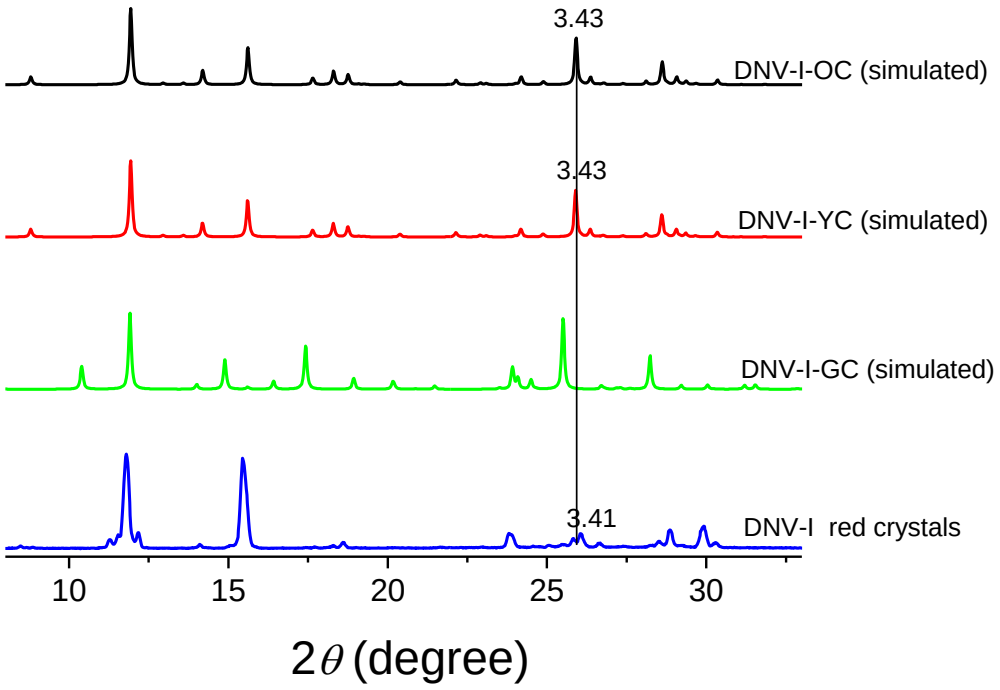

Fig. S3. Simulated and measured XRD patterns of **DNV-I** crystals

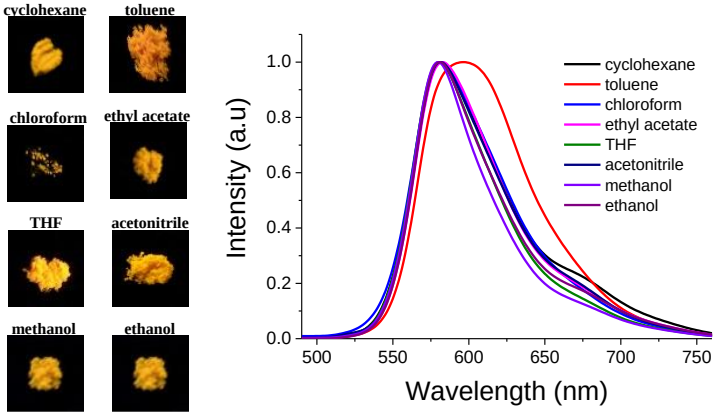

Fig. S4 Fluorescence images and spectra of **MBAV-I** obtained by recrystallization from different solvents

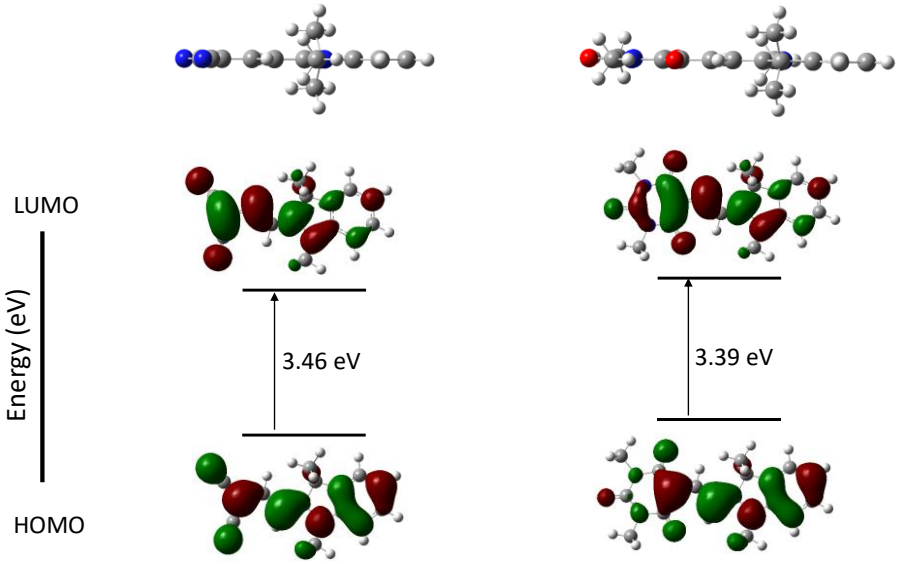

Fig. S5. Conformation, energy levels and molecular orbital surfaces in the optimized structures by DFT calculation at the B3LYP/6-31G (D,P) level

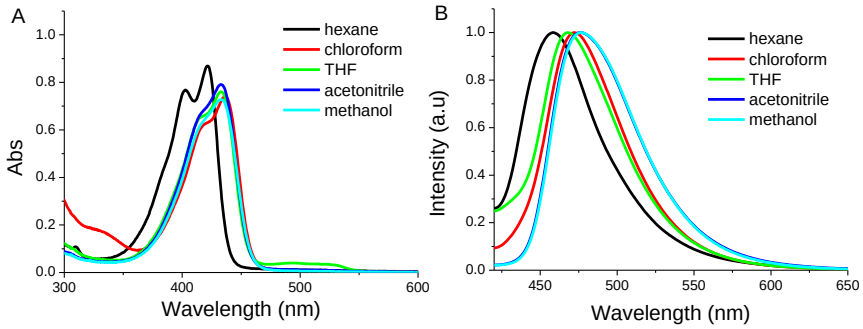

Fig. S6. (A) Absorption and (B) fluorescence spectra of **DNV-I** in various solvents (1.0×10^{-5} M)

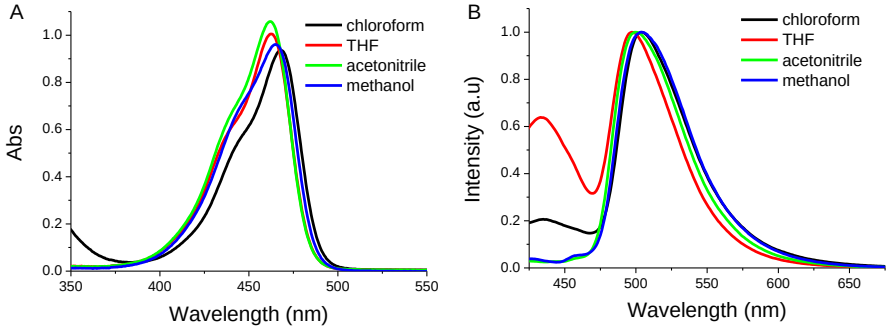

Fig. S7. (A) Absorption and (B) fluorescence spectra of **MBAV-I** in various solvents (1.0×10^{-5} M)

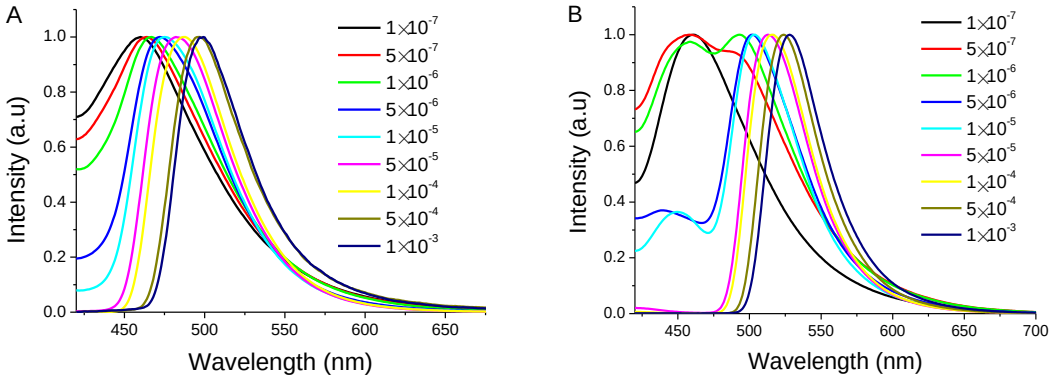

Fig. S8. Normalized fluorescent spectra of **DNV-I** (A), and **MBAV-I** (B) in chloroform with different concentrations from 10^{-7}~10^{-3}mol/L

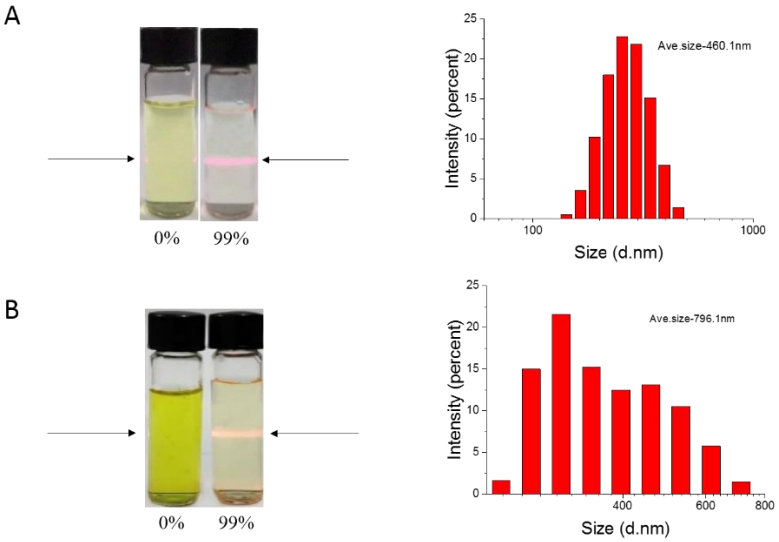

Fig. S9. Tyndall effect and size distribution (f_w 99%) of **DNV-I** (A) and **MBAV-I** (B)

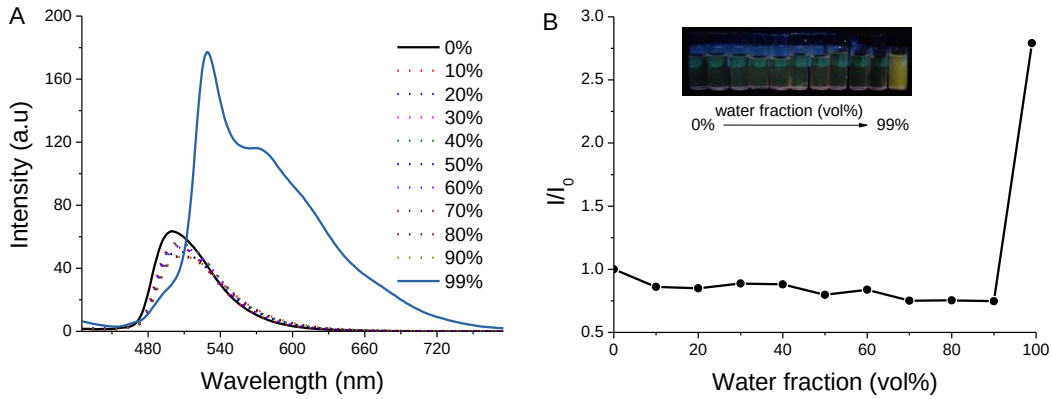

Fig. S10. (A) Fluorescent spectral changes and (B) relative fluorescent intensity change (I/I_0) of **MBAV-I** in acetonitrile/H_2O with f_w= 0-99% (λ_{ex} = 470 nm). The inset shows the fluorescent images with different f_w under 365 nm light irradiation (1.0×10^{-5} M).

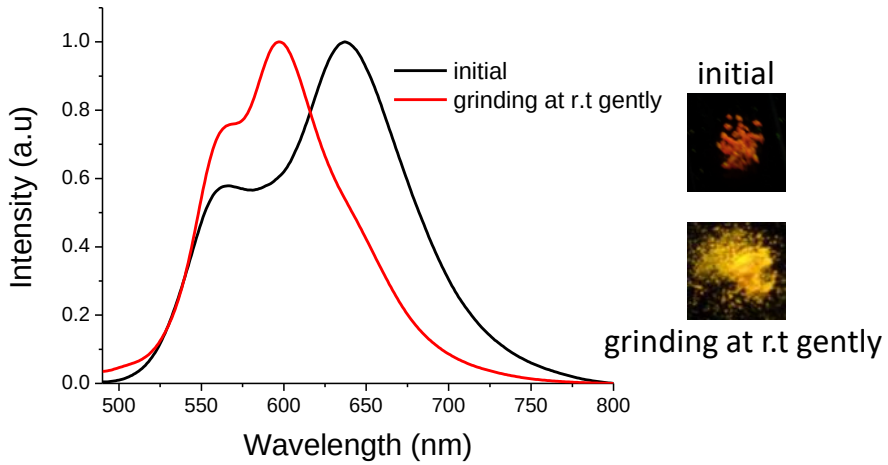

Fig. S11. The fluorescent spectra and images of **DNV-I** upon grinding gently at room temperature

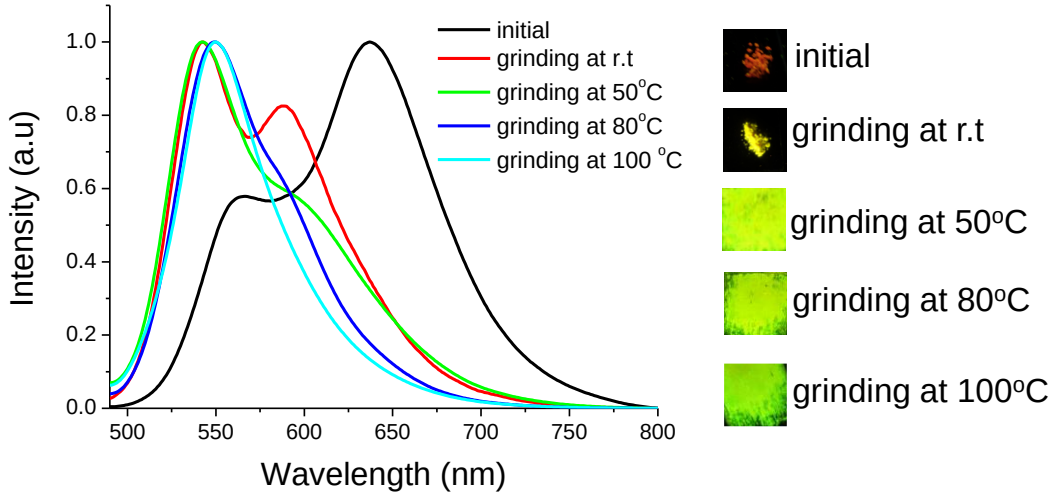

Fig. S12. The fluorescent spectra and images of **DNV-I** upon grinding at different temperatures

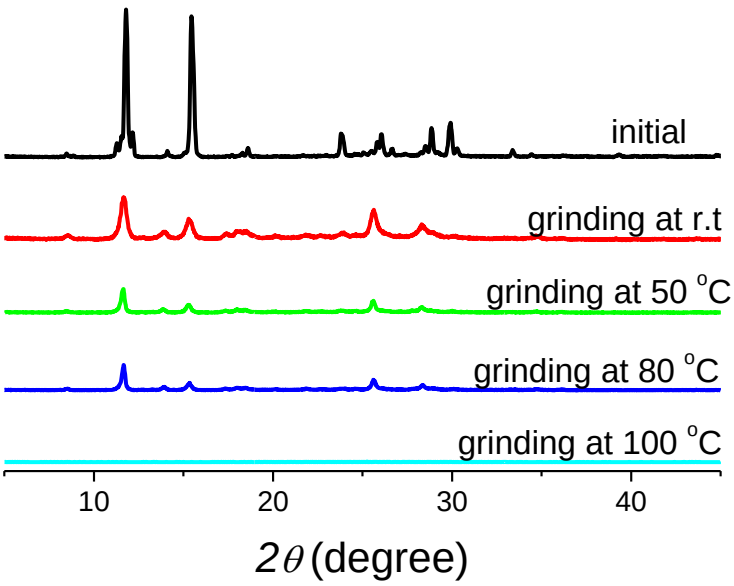

Fig. S13. XRD patterns of **DNV-I** upon grinding at different temperatures

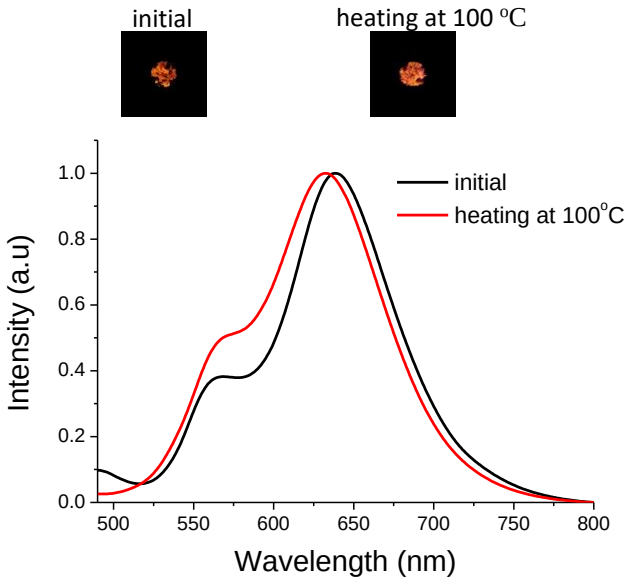

Fig. S14. Fluorescent spectra and images of the initial state of **DNV-I** upon thermal treatment

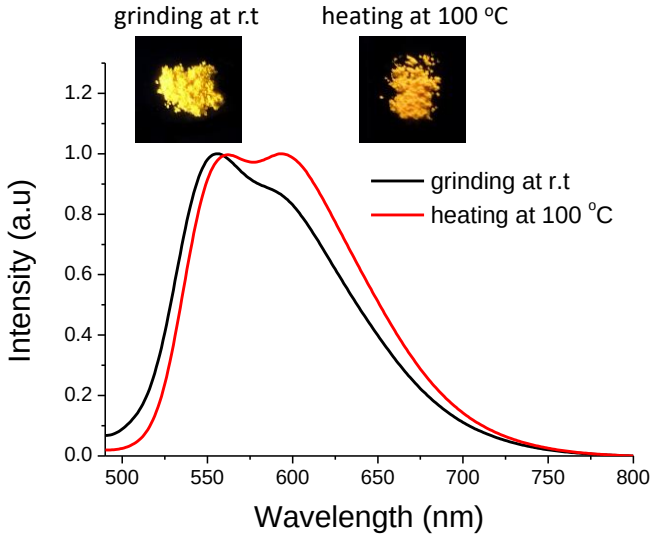

Fig. S15. Fluorescent spectra and images of ground sample **DNV-I** (grinding at r.t), followed by heating at 100 °C, then cooling to room temperature.

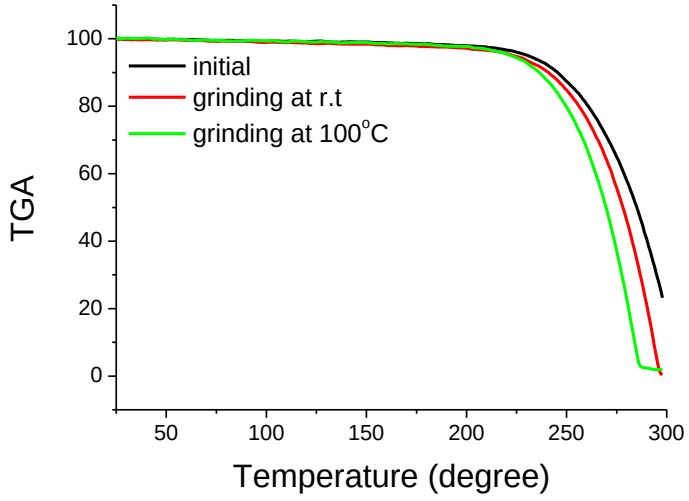

Fig. S16. TGA curves of the initial and ground sample.

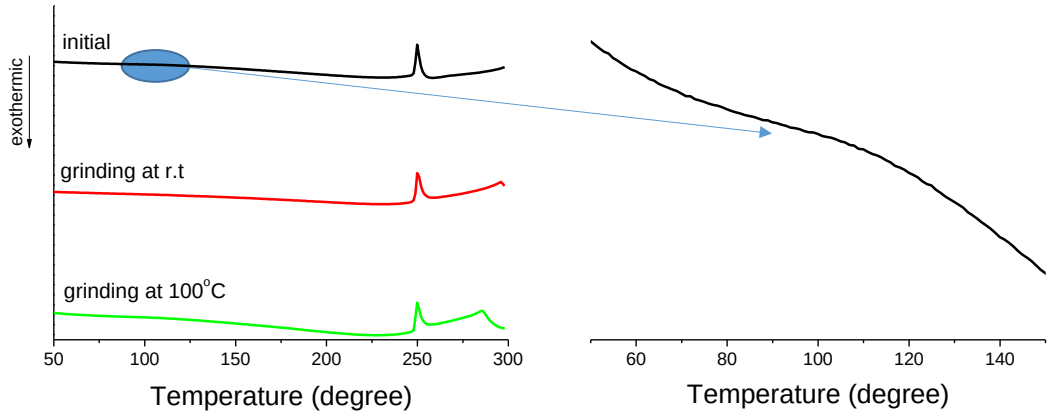

Fig. S17. DSC curves of the initial and ground sample (Left: full curve; right: amplified curve for the initial sample).

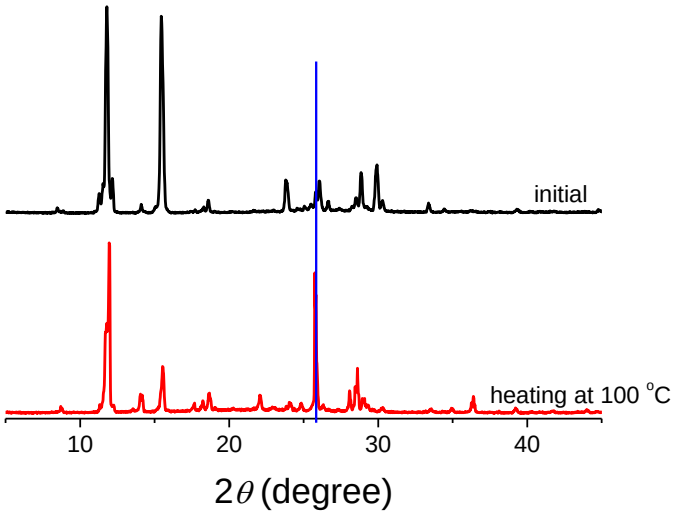

Fig. S18. XRD patterns of **DNV-I** measured at room temperature before and after heating

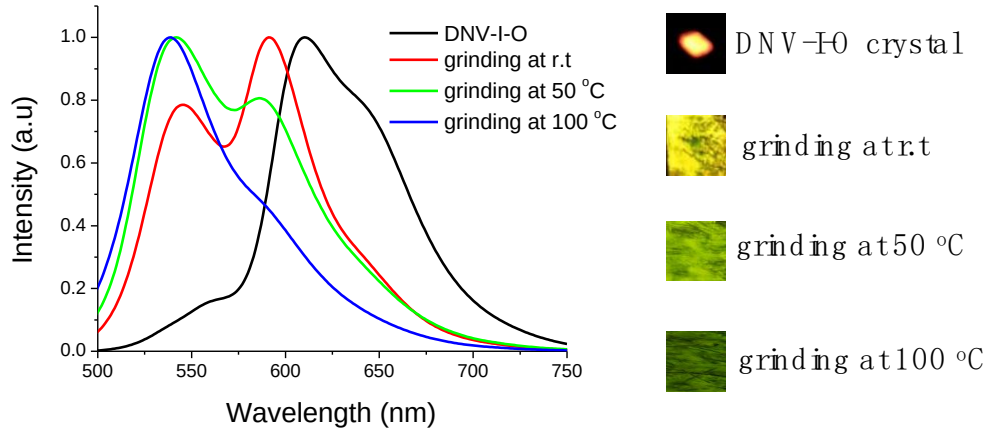

Fig. S19. Fluorescent spectra and images of the crystal **DNV-I-OC** upon grinding at different temperature

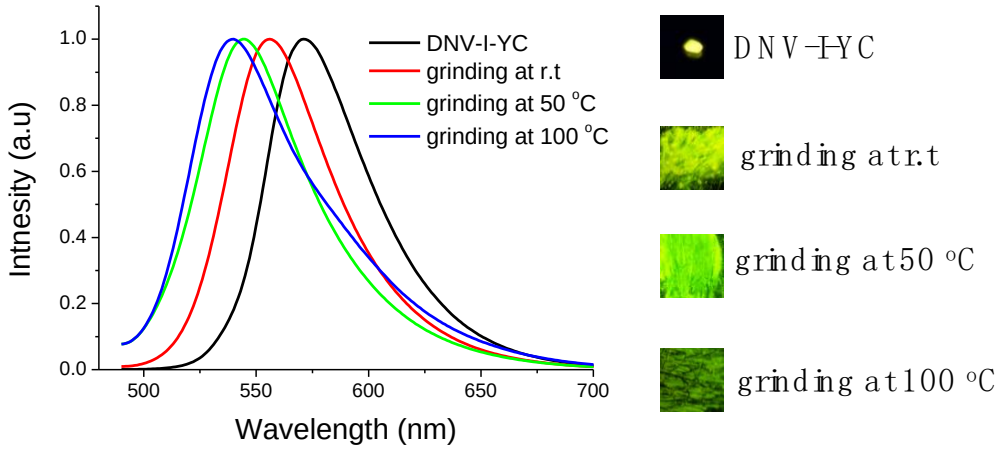

Fig. S20. Fluorescent spectra and images of the crystal **DNV-I-YC** upon grinding at different temperature

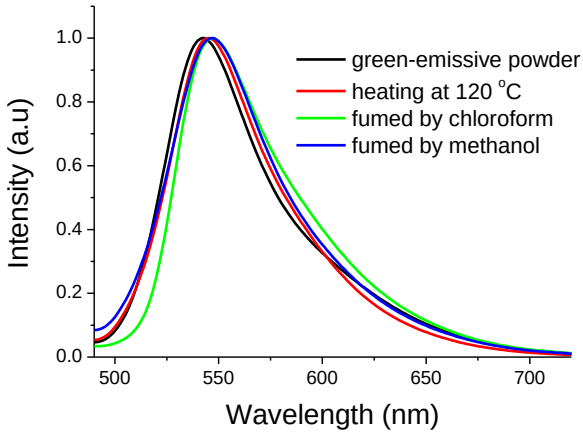

Fig. S21. Fluorescent spectra of the green-emissive **DNV-I** sample upon external stimuli

Table S3. Photophysical data of **DNV-I**, and **MBAV-I** in different solid states

compound	state	λ_{em} (nm)	$\tau_1/\tau_2/\tau_3$(ns)[a], A_1[b]/A_2[b]/A_3[b] (%)	<τ> (ns)[c]	Φ_F (%)
DNV-I	initial	555	1.37,2.96,9.53(41/54/5)	2.64	26.72
		637	4.42,11.44(88/12)	5.26	
	grinding at r.t	540	0.68,2.37(50/50)	1.53	15.41
		585	2.50,7.31(45/55)	5.15	
	grinding at 100°C	542	0.80,2.36(55/45)	1.50	11.98
MBAV-I	initial	578	0.85,2.31(70/30)	1.29	23.66
	ground	574	0.84,2.32(70/30)	1.29	32.11

[a] Fluorescence lifetime, [b] Fractional contribution, [c] Weighted mean lifetime.

Table S4. Photophysical data of crystals of **DNV-I**

crystal	λ_{em} (nm)	$\tau_1/\tau_2/\tau_3$(ns)[a], A_1[b]/A_2[b]/A_3[b] (%)	<τ> (ns)[c]	Φ_F (%)
2113793	560(s)	1.65,5.05(75/25)	2.50	68.33
	610	5.28,39.73(92/8)	8.04	
	640	5.3(100)	5.25	
2113802	571	4.12, 9.12 (25/7)	7.87	43.70
2132410	538	3.04,14.69(96/4)	3.51	35.23

[a] Fluorescence lifetime, [b] Fractional contribution, [c] Weighted mean lifetime.

4. Crystal data

Table S5. Crystal data and structure refinements of the **DNV-I** crystals

CCDC number	2113793	2113802	2132410
Empirical formula	$C_{16}H_{15}N_3$	$C_{16}H_{15}N_3$	$C_{16}H_{15}N_3$
Formula weight	249.31	249.31	249.31
Temperature/K	298	298	298
Wavelength/Å	1.54184	1.54184	1.54184
Crystal system	orthorhombic	orthorhombic	monoclinic
Space group	*Pnma*	*Pnma*	$P2_1/m$
a/Å	13.6543(4)	13.6604(3)	8.6221(2)
b/Å	18.9539(3)	6.8744(2)	6.9789(2)
c/Å	20.6072(3)	14.8177(3)	11.5076(3)
α/°	90	90	90
β/°	90	90	99.602(2)
γ/°	90	90	90
Volume/Å^3	1390.01(7)	1391.49(6)	682.74(3)
Z	4	4	2
ρ_{calc}g/cm^3	1.191	1.190	1.213
Reflections collected	13710	3943	3807
Independent reflections	1527	1497	1466
R(int)	0.0652	0.0257	0.0354
R(sigma)	0.0273	0.0334	0.0343
GOF	1.085	1.044	1.014
R1 [I>=2σ (I)]	0.0683	0.0491	0.0519
wR2 [I>=2σ (I)]	0.1566	0.1283	0.1399
R1 (all data)	0.0702	0.0541	0.0545
wR2 (all data)	0.1585	0.1331	0.1444

5. NMR spectra

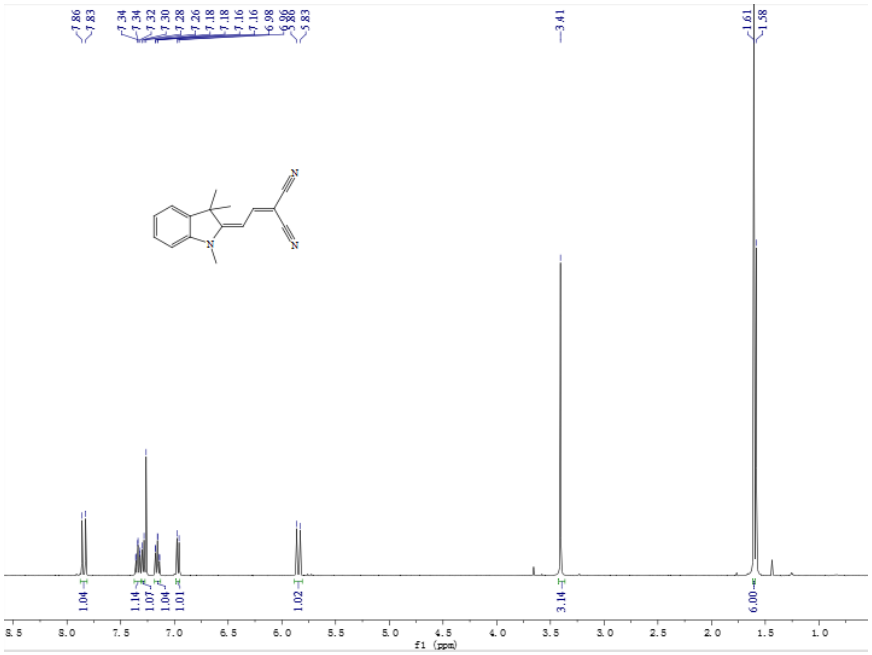

Figure S22. ^{1}H NMR of **DNV-I** (400 MHz, $CDCl_3$)

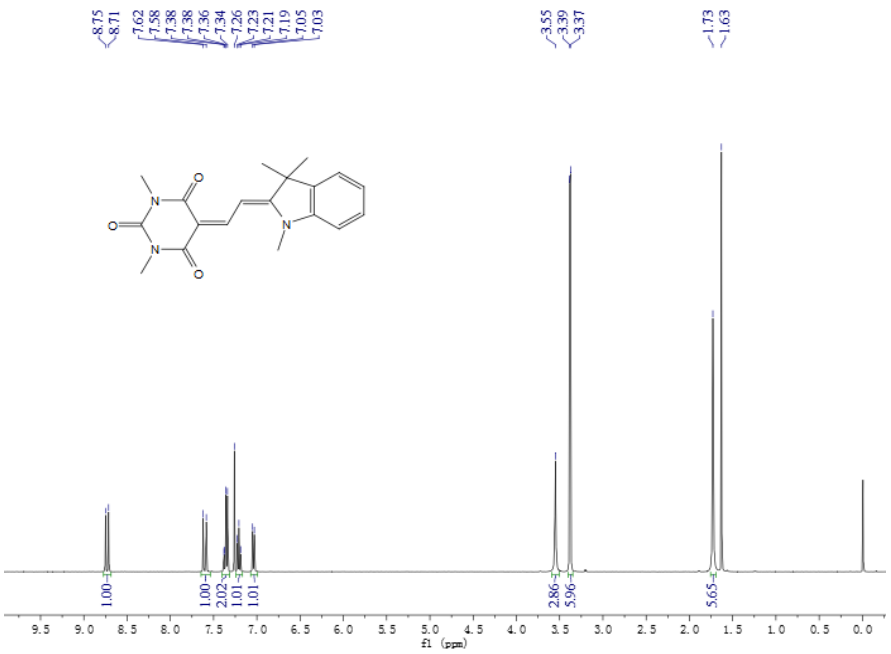

Figure S23. ^{1}H NMR of **MBAV-I** (400 MHz, $CDCl_3$)

6. References

[1] (a) C. Reidlinger, R. Dworczak, H. Junek. Dyes Pigments, 2000, 44, 219-226; (b) A. V. Kulinich, A. A. Ishchenko, S. V. Shishkina, I. S. Konovalova, O. V. Shishkin. *J. Struct. Chem*., 2007, 48, 914-921.

[2] (a) A. V. Kulinich, N. A. Derevyanko, A. A. Ishchenko. *Russ. J. Gen. Chem*., 2006, 76, 1441-1457; (b) F. Wurthner. *Synthesis*, 1999, 2103-2113; (c) A. A. Ishchenko, A. V. Kulinich, S. L. Bondarev, V. N. Knyukshto. *Russ. J. Gen. Chem*., 2007, 77, 1787-1798.